



THE UNIVERSITY *of* EDINBURGH

Edinburgh Research Explorer

Photonic crystal fibre as an optofluidic reactor for the measurement of photochemical kinetics with sub-picomole sensitivity

Citation for published version:

Williams, GOS, Chen, JSY, Euser, TG, Russell, PSJ & Jones, AC 2012, 'Photonic crystal fibre as an optofluidic reactor for the measurement of photochemical kinetics with sub-picomole sensitivity', *Lab on a Chip*, vol. 12, no. 18, pp. 3356-3361. <https://doi.org/10.1039/c2lc40062f>

Digital Object Identifier (DOI):

[10.1039/c2lc40062f](https://doi.org/10.1039/c2lc40062f)

Link:

[Link to publication record in Edinburgh Research Explorer](#)

Document Version:

Peer reviewed version

Published In:

Lab on a Chip

Publisher Rights Statement:

Copyright © 2012 by the Royal Society of Chemistry. All rights reserved.

General rights

Copyright for the publications made accessible via the Edinburgh Research Explorer is retained by the author(s) and / or other copyright owners and it is a condition of accessing these publications that users recognise and abide by the legal requirements associated with these rights.

Take down policy

The University of Edinburgh has made every reasonable effort to ensure that Edinburgh Research Explorer content complies with UK legislation. If you believe that the public display of this file breaches copyright please contact openaccess@ed.ac.uk providing details, and we will remove access to the work immediately and investigate your claim.



Post-print of a peer-reviewed article published by the Royal Society of Chemistry.

Published article available at: <http://dx.doi.org/10.1039/C2LC40062F>

Cite as:

Williams, G. O. S., Chen, J. S. Y., Euser, T. G., Russell, P. S. J., & Jones, A. C. (2012). Photonic crystal fibre as an optofluidic reactor for the measurement of photochemical kinetics with sub-picomole sensitivity. *Lab on a Chip*, 12(18), 3356-3361.

Manuscript received: 13/01/2012; Accepted: 08/06/2012; Article published: 06/07/2012

Photonic Crystal Fibre as an Optofluidic Reactor for the Measurement of Photochemical Kinetics with Sub-Picomole Sensitivity**

Gareth O.S. Williams,¹ Jocelyn S.Y. Chen,² Tijmen G. Euser,² Philip St.J. Russell² and Anita C. Jones^{1,*}

^[1]EaStCHEM, School of Chemistry, Joseph Black Building, University of Edinburgh, West Mains Road, Edinburgh, EH9 3JJ, UK.

^[2]Max Planck Institute for the Science of Light, Günther-Scharowsky-Str. 1/Bldg. 24, 91058 Erlangen, Germany.

^[*]Corresponding author; e-mail: a.c.jones@ed.ac.uk, fax: +44(0)1316504753

^[**]This work forms part of a project funded by the Koerber Foundation. G.O.S.W. and A.C.J. also acknowledge the UK EPSRC for funding. G.O.S.W. acknowledges programming support from G.J.H. Williams.

Supporting information:

† Electronic supplementary information (ESI) available. See <http://dx.doi.org/10.1039/C2LC40062F>

Abstract

Photonic crystal fibre constitutes an optofluidic system in which light can be efficiently coupled into a solution-phase sample, contained within the hollow core of the fibre, over long path-lengths. This provides an ideal arrangement for the highly sensitive monitoring of photochemical reactions by absorption spectroscopy. We report here the use of UV/vis spectroscopy to measure the kinetics of the photochemical and thermal *cis-trans* isomerisation of sub-picomole samples of two azo dyes within the 19- μm diameter core of a photonic crystal fibre, over a path length of 30 cm. Photoisomerisation quantum yields are the first reported for “push-pull” azobenzenes in solution at room temperature; such measurements are challenging because of the fast thermal isomerisation process. Rate constants obtained for thermal isomerisation are in excellent agreement with those established previously in conventional cuvette-based measurements. The high sensitivity afforded by this intra-fibre method enables measurements in solvents in which the dyes are too insoluble to permit conventional cuvette-based measurements. The results presented demonstrate the potential of photonic crystal fibres as optofluidic elements in lab-on-a-chip devices for photochemical applications.

Introduction

The application of photochemistry is seeing growth in many areas, including photo-medicine¹, artificial photosynthesis^{2,3}, optically switchable media for data storage⁴ and the control of molecular machines⁵, stimulating the synthesis and characterisation of novel photoactive compounds. There is also a drive for the miniaturisation and integration of sample preparation and monitoring systems into lab-on-a-chip devices. This approach can be applied to photochemical reactions by utilising optofluidic systems, in which optical excitation and detection systems are integrated with microfluidics.⁶ UV/visible (UV/vis) absorption spectroscopy is a convenient and commonly used method for monitoring the progress of photochemical reactions in conventional cuvette-based measurements, but is relatively insensitive because of the short path-lengths that are typically used. Increasing the path-length is often impractical because of the constraints of commercial spectrometers or the limited availability of sample. The use of glass capillaries reduces the required sample volume but simple capillaries have very high optical losses and are highly sensitive to bending, greatly limiting the possible length that can be used⁷. The ideal sample cell for the spectroscopic study of photochemical reactions is an optofluidic device that combines a long path-length with a small cross-sectional area, in which the entire (small) sample volume is exposed to both the photochemical excitation (pump) beam and the spectroscopic probe beam. These requirements are hard to achieve in conventional lab-on-a-chip designs^{8,9,10}.

Integration of lasers and a micro-cuvette on a chip has been achieved¹¹ and provides small volumes, but, as the sample was not contained within a waveguide, the distance over which it could be excited was limited to $\sim 1\text{mm}$. Other systems have used liquid core waveguides with guidance through a metal jackets¹². These designs

experience high loss due to surface, reducing guidance and limiting the path length that can be used.

Progress in implementing long path-length absorption spectroscopy in an optofluidic system has been made through the use of photonic crystal fibre (PCF). In a PCF, light is trapped inside the fibre core by a periodic wavelength-scale lattice of microscopic holes in the cladding glass, a “photonic crystal”¹³. Initial studies were performed using solid-core PCF (SC-PCF), a fibre with a solid silica core surrounded by a lattice of air holes producing the cladding crystal structure. The sample is infiltrated into the cladding of the fibre and probed by the evanescent field of the light guided through the core^{14,15}. For example, Cordeiro *et al* showed enhanced absorption sensitivity for Methylene Blue dye using a micro-structured fibre core¹⁶, whilst Euser *et al* demonstrated the use of a suspended-core fibre for absorption sensing of aqueous NiCl₂ with a sensitivity two orders of magnitude greater than in conventional systems¹⁷. Whilst SC-PCF is effective in achieving detection over long path-lengths, there is limited overlap between the guided light and the sample, providing a less-than-ideal probe regime. Furthermore, the probed sample is in very close proximity to the silica fibre surface, where its properties may differ from those in the bulk solution. These disadvantages are overcome by the use of hollow-core PCF (HC-PCF), in which light is guided through the sample solution in the hollow core of the fibre.

The structure of the kagomé HC-PCF used in this study, shown in Figure 1(C) and (D), allows the guidance of light, in a single well-defined mode, over long path-lengths through the core region. When the fibre microstructure is filled with a sample solution there is near perfect light-sample overlap within the fibre core^{18,19}. The dimensions of the kagomé PCF are compared to a standard 1-cm cuvette in Figure 1(A) and (B). Irradiation across the full width of the cuvette, over a path-length of 1cm, requires a minimum sample volume of 1 ml, whereas the 19- μ m core of the HC-PCF holds only 3 nl per cm of path-length. In the present work, a 30-cm length of fibre was used, containing a sample volume of 90 nl. Both excitation and broadband measurement sources can be co-coupled into the fibre core, giving excellent overlap of both with the sample (Fig. 1(E) and (F)). Furthermore, precise knowledge of the excitation intensity and probed volume facilitates quantitative modelling of the kinetics of a photochemical reaction taking place within the fibre. The kagomé HC-PCF used in these experiments exhibits losses of $\sim 1\text{dBm}^{-1}$ allowing, in principle, several metres of fibre to be used before loss hinders measurements. Moreover, this fibre type supports broadband guidance, permitting measurement of the complete visible absorption spectra of the azo dyes studied here.

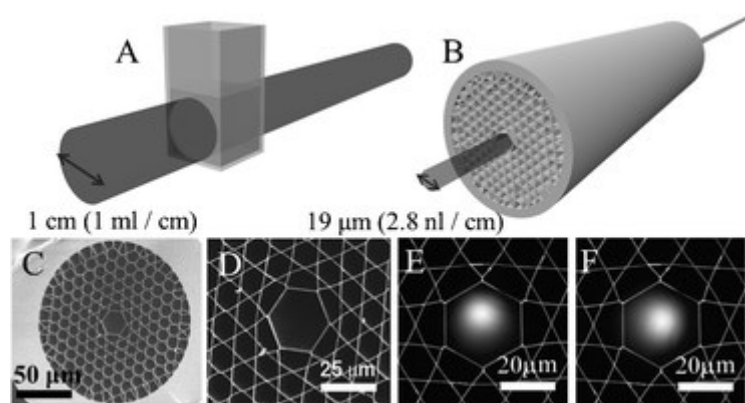


Figure 1. Schematic comparison of the irradiated sample volumes in a conventional cuvette (A) and a HC-PCF (B). High-resolution scanning electron micrographs of a kagomé HC-PCF with a core diameter of 19 μm (C-D). Transverse irradiance profile measured using the 488-nm laser (E) and the broadband xenon lamp (F).

Previously, we have demonstrated the use of HC-PCF as a photochemical reactor to monitor the photolysis of vitamin B12, cyanocobalamin, an irreversible reaction with very low quantum yield ($\sim 10^{-4}$)²⁰. The strong confinement of both sample and light in the hollow core resulted in a 1000-fold increase in reaction rate over that in a conventional cuvette. We now report the extension of this approach to the measurement of the kinetics of thermally reversible photochemical reactions with relatively high quantum yield, the photoisomerisation of azo dyes. The spectroscopic monitoring of such reactions poses challenges that were not encountered in our previous study. The thermal reversibility demands that the spectroscopic measurement is near-simultaneous with the photochemical excitation and the high quantum yield requires the use of a low probe intensity to avoid probe-induced photochemistry.

We note that the photogeneration and detection of transient species within a HC-PCF has been reported previously by Khetani *et al*, using laser flash photolysis²¹. However, they used a perpendicular arrangement of pump and probe beams, such that the sample solution was excited perpendicular to the fibre core, through the cladding, and monitored by probe light guided through the core. Thus, the path-length for pump beam was extremely short, only a few microns (the diameter of the fibre core), requiring the use of a concentrated (mM) sample solution, and the effective probe path length was only ~ 1 cm. This study, therefore, failed to exploit the large gain in sensitivity offered by coaxial guiding of both pump and probe beams through the hollow core. Also, the cladding holes of the fibre used were collapsed, affecting the guidance mechanism of the fibre. When the cladding holes are collapsed, the core of the fibre has a higher effective refractive index than the cladding and guides by the mechanism of total internal reflection. The relatively large diameter of the core means that a high number of modes are supported and single-mode guidance is very hard to achieve.

Two azobenzene-based dyes, Disperse Red 1 (DR1), N-ethyl-N-(2-hydroxyethyl)-4-(4-nitrophenylazo)aniline, and Disperse Orange 1, 4-anilino-4'-nitroazobenzene, were chosen for the present study. The structures of the dyes, together with the *cis-trans* isomerisation reaction are shown in Fig. 2.

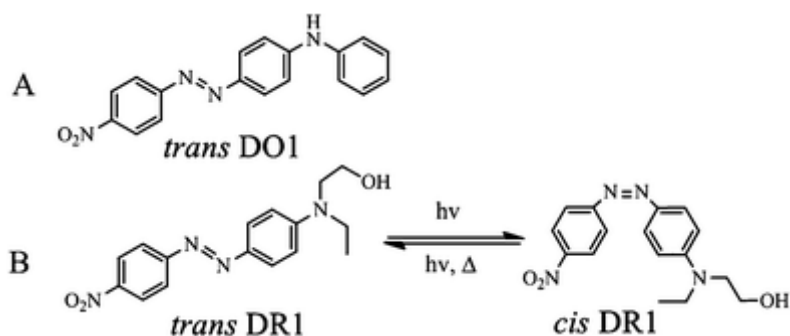


Figure 2. (A) Structure of *trans* Disperse Orange 1; (B) the reversible isomerisation of Disperse Red 1, from *trans* (left) to *cis* (right); $h\nu$ indicates a photochemical process and Δ a thermal process.

The isomerisation of azobenzene and its derivatives is considered a paradigm of unimolecular photochemistry, and the kinetic model is well-established, as briefly summarised here. The *trans* isomer is the thermally stable species and the un-irradiated dye exists exclusively in this form. Irradiation, by either UV or visible light, induces reversible photoisomerisation, such that an equilibrium between *trans* and *cis* forms, known as the photostationary state (PSS), is attained. There is a high thermal barrier to the forward process which, therefore, only occurs photochemically, but the reverse process occurs both photochemically and thermally. The photoisomerisation of azo dyes is typically accompanied by a colour change (photochromism), allowing the process to be monitored by absorption spectroscopy^{22,23,24,25,26,27}. The dyes studied here belong to a particular class of azobenzene derivative known as “push-pull” azobenzenes. These contain electron donating and electron accepting substituents at the 4 and 4' positions, respectively, *para* to the azo bond. This substitution increases electron delocalisation, affecting the ordering of the excited state energy levels and shifting the most intense electronic transitions into the visible part of the spectrum. A further consequence of this substitution is an acceleration of the rate of thermal *cis*-to-*trans* isomerisation and a strong dependence of this rate on solvent polarity²⁸. Measuring the photoisomerisation quantum yields of push-pull azobenzenes is challenging because of the fast thermal isomerisation and we are not aware of any previous measurements in solution at room temperature. A very recent review²⁸ cites only one study²⁹, carried out at low temperature to prevent the thermal process.

Azo dyes have long been used as dyes and colorants³⁰, but more recent applications seek to exploit the ability to reversibly photoswitch the geometric, electronic and optical properties of the molecule. Such applications include memories and switches in new electronic and photonic systems^{31,32}, optical control of various physical

properties of materials^{33,34} and optically switchable components in molecular machines³⁵ and biomolecules³⁶. Measurement of the kinetics of azo isomerisation is central to the design and optimisation of optical switching characteristics for specific applications.

Experimental

The photonic crystal fibre was fabricated in-house at the Max Planck Institute for the Science of Light. Disperse Red 1 and Disperse Orange 1 were purchased from Sigma Aldrich and used as received. All solvents were of HPLC grade.

The experimental system is shown in Fig. 3. A 488-nm diode laser (photochemical pump) and a broadband xenon lamp (spectroscopic probe) are co-coupled into a 30 cm length of the HC-PCF, via an endlessly-single-mode fibre, to ensure both have the same modal properties. This enables spectroscopic measurements of precisely the same sample volume as that being excited by the laser source. Each end of the hollow core fibre is mounted in a custom-built liquid cell (Fig. 3 inset) to allow introduction of the sample solution into the fibre, via a syringe pump, whilst maintaining optical alignment and minimising dead volume. An optical window on the cell allows coupling of light into the fibre.

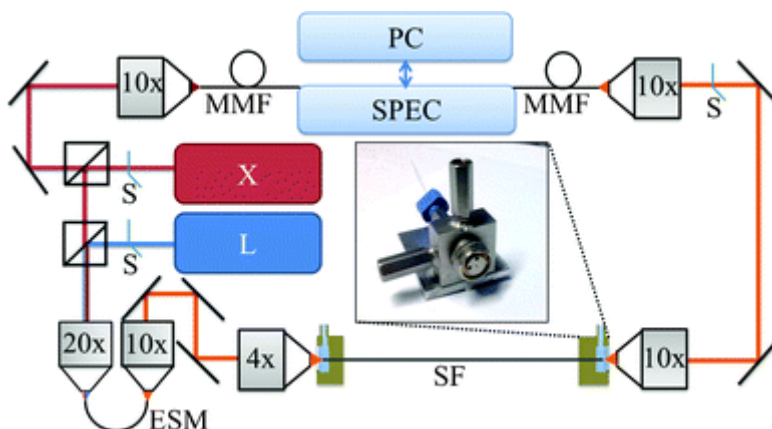


Figure 3. Schematic diagram of the experimental setup. The 488-nm diode laser (L) and the broadband xenon lamp (X) are co-aligned and coupled into a short piece of endlessly single mode fibre (ESM) for spatial filtering, before being coupled into the HC-PCF containing the sample (SF). The transmitted light and a reference beam (directly from the xenon lamp) are delivered, via multimode fibres (MMF), to the dual-channel spectrometer (SPEC) interfaced to a PC. The laser and lamp outputs and the input to the spectrometer are controlled by electronic shutters (S). The inset shows the fluid cell through which the sample solution is introduced into the core of the fibre.

The pump wavelength lies within the probed spectral region, so saturation of the spectrometer by the relatively intense pump laser must be avoided. Therefore, electronic shutters, controlled by the PC, are used to implement a sequential pump-probe technique. A reference spectrum of the lamp is acquired for each measurement to correct for any instability in the probe source. Measurements and shutter control are automated using a Matlab computer program, allowing the photoisomerisation process to be monitored by acquisition of the complete absorption spectrum on the 10s of millisecond timescale.

The experimental photoisomerisation data are fitted numerically by a kinetic model with three variable parameters, the rate constants for the three isomerisation processes: *trans*-to-*cis* photoisomerisation, *cis*-to-*trans* photoisomerisation and *cis*-to-*trans* thermal isomerisation. The precisely defined excitation conditions make measurement of the irradiation intensity straightforward, without the use of actinometry, which is necessary in cuvette-based experiments. The kinetic model is described in detail in the Supplementary Information. The model takes account of the fall-off in excitation intensity along the length the fibre, due to both absorption and the intrinsic fibre losses. For measurements in the pump-probe mode, the model also allows for the occurrence of thermal relaxation from *cis* to *trans* isomer during the probe periods, when the excitation laser is off. The rate constant for thermal *cis* to *trans* isomerisation is determined independently by monitoring the reverse reaction from the PSS in the absence of irradiation; this value is then fixed in the model. Application of the model to the photoisomerisation data returns the value of the photoisomerisation quantum yield.

Measurements were carried out on both dyes in cyclohexane and toluene. DR1 was also measured in pentane, a solvent in which the dye is highly insoluble, precluding conventional cuvette-based measurement. The 30-cm path-length permitted use of dye concentrations as low as 1 μM corresponding to less than 100 fmol of dye in the measurement volume of 90 nL.

Results and Discussion

As shown in Fig. 4, photoisomerisation of *trans* DR1 results in a decrease in intensity of the visible absorption band between 400 and 550 nm. Similar behaviour is seen for DO1. Fig. 4 compares spectra recorded for a 100 μM solution in a 1-cm cuvette (in a conventional UV/vis spectrometer) with those measured for a 5 μM solution in a 30-cm PCF. The spectral profiles are in good agreement; however, the absorbance measured in the PCF is somewhat lower than that predicted on the basis of the Beer-Lambert law. This can be attributed to adsorption of dye molecules to the fibre walls, where there are not exposed to guided light, which reduces the effective sample concentration. Allowing the sample to flow through the fibre saturates the surface and the recorded absorbance approaches that predicted. There is the potential to use surface-functionalised fibres to inhibit adsorption.

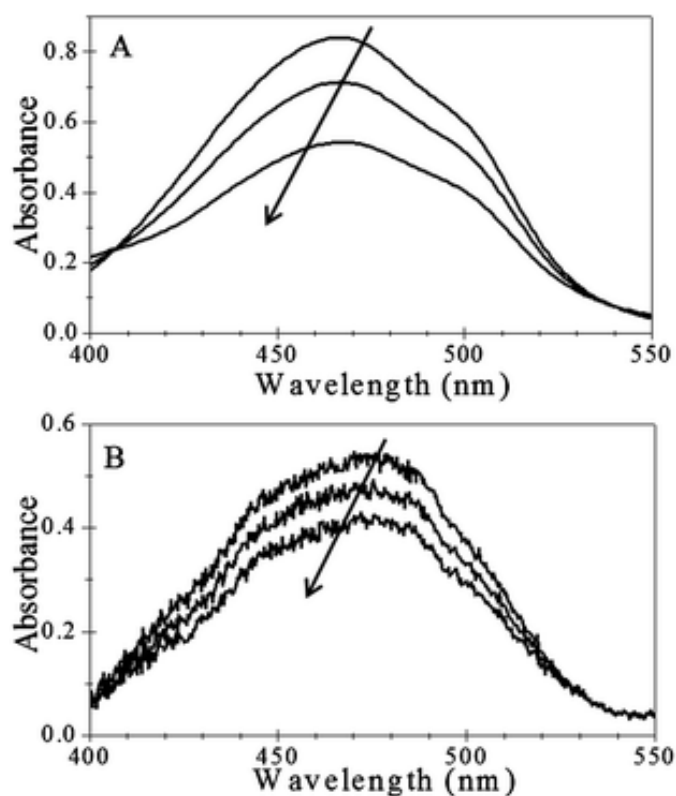


Figure 4. Absorption spectra of Disperse Red 1 in toluene measured during photoisomerisation in (A) a 1-cm cuvette, at 100 μM (in a UV/vis spectrometer, scan time 45 s) and (B) in a 30-cm kagomé PCF at 5 μM (acquisition time 500 ms). The arrow indicates the direction of photoisomerisation from the *trans* to the *cis* isomer.

As a result of the tight confinement of the guided light in the core of the sample fibre, very low source powers are needed to produce sufficient power density to induce the photochemical process. Consequently, the low-power broadband xenon lamp, intended for use as the spectroscopic probe source, can produce photoisomerisation. This is illustrated in Fig. 5(A), which shows the effect of low-power irradiation of a 5 μM cyclohexane solution of DO1. At a lamp power of approximately 1 μW , the PSS is attained in less than 10 s. At this power, the sample absorption is saturated and no further increase in rate is seen with increasing power. As the power is decreased, the rate of attainment of the PSS decreases as expected. The time taken to reach the PSS is plotted as a function of incident power in Fig. 5(B), also shown for comparison is the result of a conventional cuvette measurement on the same solution. Almost three orders of magnitude more power was needed to reach the PSS in a comparable time in the cuvette: irradiation with 100 μW produced the PSS in 20 s, compared with <0.1 μW in the PCF. Although the total power entering the fibre is three orders of magnitude lower, the power density in the 19- μm fibre core is approximately three orders of magnitude higher, 60 mWcm^{-2} , compared to $\sim 50 \mu\text{Wcm}^{-2}$ for the cuvette measurement.

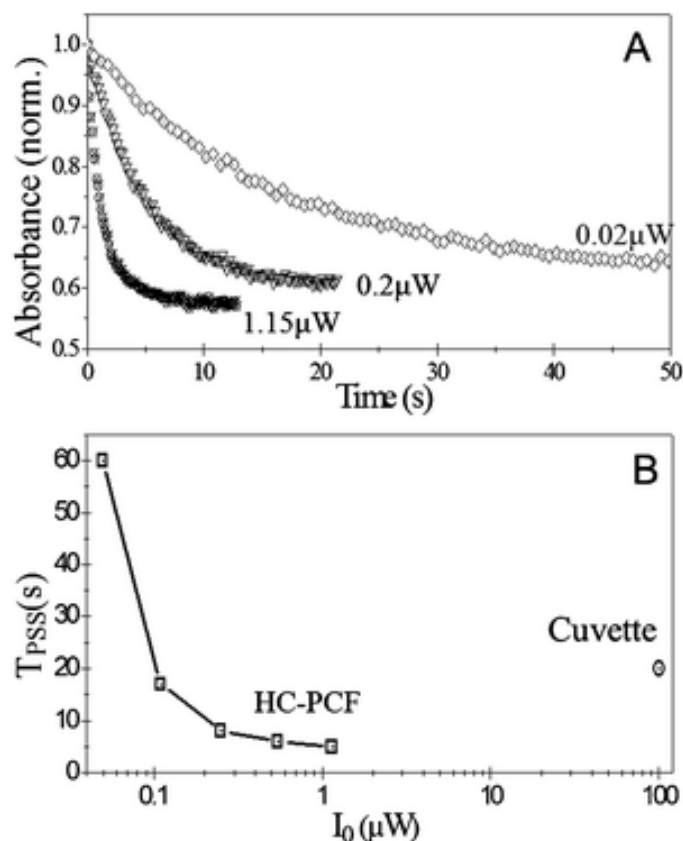


Figure 5. The effect of incident excitation power on the time taken to reach the photostationary state for Disperse Orange 1 in cyclohexane at 5 μM , in a 30-cm kagomé fibre. (A) Temporal evolution of absorbance at 470 nm for excitation powers of 1.15 μW , 0.2 μW and 0.02 μW . (B) Time taken to reach the photostationary state as a function of excitation power, I_0 . The solid line is a guide only. The isolated point is the value for an equivalent cuvette measurement.

Using the xenon lamp as both pump and probe, the photoisomerisation of DO1 was monitored on the millisecond timescale by recording the complete absorption spectrum, with an integration time of 10 ms, at 100 ms intervals. The measured temporal evolution of the absorbance at 470 nm is shown in Fig. 6 (A), together with the fitted kinetic function. Whilst this offers an attractively simple method of simultaneously exciting and probing the photoswitching process, the use of polychromatic excitation hinders modelling of the kinetics because of the need to take account of the wavelength-dependence of the irradiation intensity and the absorption cross-sections of the two isomers. In the present case, an approximate model was used in which the total incident intensity and spectrally averaged cross-sections were used. This gave an estimate of 0.23 for the *trans*-to-*cis* photoisomerisation quantum yield of DO1. To our knowledge this is the first reported measurement of this parameter.

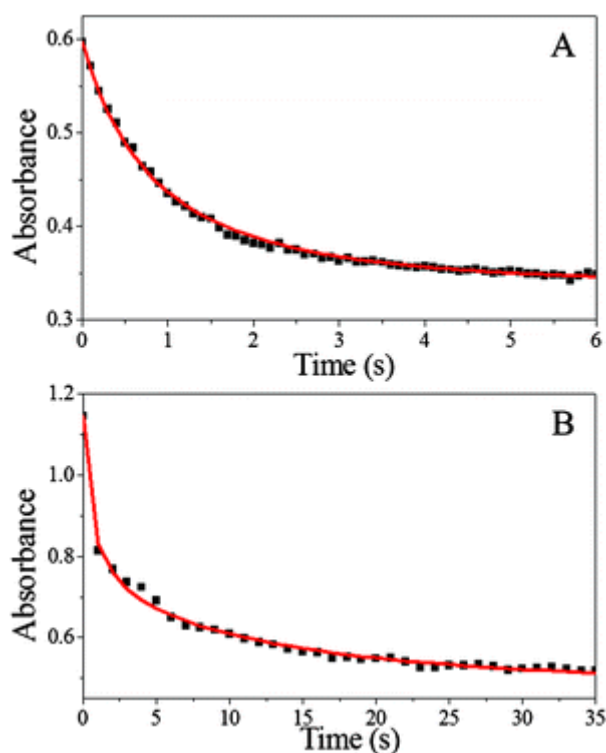


Figure 6. (A) The photoisomerisation kinetics of DO1 in toluene at a concentration of 2 μM . The experimentally measured temporal evolution of the absorbance at 470nm (■), using the broadband output of the xenon lamp as both pump and probe, and the fitted theoretical function (—). (B) The photoisomerisation kinetics of DR1 in toluene at 5 μM . The experimentally measured temporal evolution of the absorbance at 488nm (■), using the diode laser as pump and the xenon lamp as probe, and the fitted theoretical function (—).

To facilitate quantitative kinetic modelling, it is desirable to reduce the probe lamp intensity to 0.02 μW or less, so that its influence becomes negligible over the time interval (~ 500 ms) needed to acquire the absorption spectrum (see Fig. 5A), and use an independent monochromatic (or narrow-band) pump source. The results of measurement of the photoswitching kinetics of DR1 in toluene using this regime, with the 488-nm diode laser as pump, are shown in Fig. 6B. Exposure of the sample to the 488-nm beam for 300 ms was followed by acquisition of the absorption spectrum over a 500-ms interval, giving a total of 800 ms for each pump-probe measurement. Excitation at a single wavelength makes determination of the photoisomerisation quantum yield straightforward and a value of 0.19 was obtained for the *trans* to *cis* isomerisation of DR1. This is in good agreement with the value of 0.2 which was reported recently for DR1 deposited as a solid film (in which thermal isomerisation is inhibited).³⁷

We now turn to the measurement of the rate of thermal conversion of the photochemically-formed *cis* isomer to the more stable *trans* form. The temporal evolution of the absorbance, for DO1 in three solvents, during the

thermal isomerisation process is shown in Fig 7. The rate constants obtained, together with those measured for DR1, are given in Table 1. Values reported from previous conventional measurements (where available) are also presented in Table 1, for comparison.

As observed in previous studies,^{24,28,38,39}, the rate of thermal isomerisation decreases with the polarity of the solvent. The values obtained in the present experiments are in very good agreement with those from previous, conventional measurements. This demonstrates that the isomerisation process is not perturbed by containment of the solution in the PCF and confirms that the sample volume that is probed is the bulk solution, not surface-bound molecules. The low solubility of push-pull azobenzenes in non-polar solvents is problematic for cuvette-based measurements and we are not aware of any previous studies in very low polarity solvents, such as pentane; the solubility of DR1 in pentane is only 1.3 μM .

Conclusion

Hollow-core PCF is a highly effective optofluidic system for the measurement of photochemical kinetics by absorption spectroscopy. The extrusion of sub-microlitre sample volumes over path-lengths of tens of centimetres enables highly sensitive measurements on sub-picomole quantities of sample. The power of this methodology has been illustrated by its application to the reversible photoisomerisation of two push-pull azobenzenes. Although the compounds used in this study are readily available, the measurement of the isomerisation kinetics of this technologically important class of azobenzenes, using conventional cuvette-based methods, has been hindered by the rapid thermal isomerisation in polar solvents and low solubility in non-polar solvents. Judicious choice of solvent has enabled some previous conventional measurements of isomerisation rate constants which have been valuable in validating the PCF technique for quantitative kinetic measurements. Having demonstrated excellent agreement of rate constants measured for the thermal *cis-trans* isomerisation of DR1 and DO1 with available literature values, we have extended our experiments to conditions that are intractable to traditional methods.

Dye	Solvent	$k_A / 10^{-3} \text{s}^{-1}$	
		This Study	Literature
DR1	Toluene	30	35 ²⁵ , 28 ²⁶
	Cyclohexane	1.0	N/A
	Pentane	0.6	N/A
DO1	Toluene	20	N/A
	Cyclohexane	0.8	0.9 ²⁷ , 0.6 ²⁴ , 0.8 ²³

Table 1. The thermal isomerisation rate constant, k_A , for DR1 and DO1 in various solvents. Values obtained in the present study are compared with those from previous, conventional measurements.

We have exploited the ease of photometry afforded by the near-perfect overlap of both pump and probe light with the sample, within the hollow core of PCF, to make the first measurement of the *trans-cis* photoswitching quantum yield of a push-pull azobenzene in solution at room temperature. The very few, previous measurements of quantum yield have used low temperature or solid samples to inhibit thermal isomerisation. The photochemical quantum yield is a crucial parameter and the ability to measure this on a small quantity of sample under ambient conditions is highly advantageous.

The sensitivity afforded by the long (30-cm) path-length of the PCF enabled the first measurement of the thermal rate constant of a push-pull azobenzene in a highly non-polar solvent, pentane, in which the solubility is very low. A concentration of 1 μM was used, equivalent to less than 100 femtomoles of DR1 in the measurement volume. Knowledge of the isomerisation rate constant under conditions of minimal solvent interaction is essential for understanding the influence of molecular environment on the mechanism of the reaction. Experimental values of thermal isomerisation rate constants in non-interacting solvents are particularly valuable for validating quantum chemical calculations, which typically consider isolated molecules in the gas phase. Recent calculations^{26,40} predict rate constants in the region of 5-10 s^{-1} for push-pull azobenzenes, more than an order of magnitude greater than the value measured here for DR1 in pentane. This highlights the need for the inclusion of realistic solvation effects in computational models.

The impact of photochemistry in the physical, biological and medical sciences, and in many modern technologies has increased greatly in recent years. New photoactive compounds are emerging in increasing numbers from synthetic chemistry laboratories, with a view to exploiting light-driven molecular processes in applications ranging from diagnostics and phototherapy to the harnessing of solar energy for green synthesis, water splitting, molecular photovoltaics and the capture and reduction of CO_2 . There is undoubtedly a demand for micro-analysis systems capable of delivering comprehensive, quantitative photochemical characterisation of the small sample quantities typically available from research-scale synthesis. The incorporation of PCFs as photochemical reactors in lab-on-a-chip devices could satisfy this need and revolutionise high-throughput screening of photoactive targets. There is also the attractive prospect of implementing photochemistry-based assays in micro-total-analysis systems; for example, combining light-controlled release of photocaged probes or analytes with highly sensitive spectroscopic detection. On the technical side, the development of a robust, easy-to-use, all-fibre optofluidic photoreactor can be envisaged, in which fibre lasers and/or PCF-based supercontinuum sources, as pump and probe, are integrated with the sample-containing PCF.

References

- [1] D. Phillips, *Photochem. Photobiol. Sci.*, 2010, **9**, 1589–1596.
- [2] D. Gust, T. A. Moore and A. L. Moore, *Acc. Chem. Res.*, 2009, **42**, 1890-1898;
- [3] J. S. Lee, S. H. Lee, J. H. Kim and C. B. Park, *Lab Chip*, 2011, **11**, 2309-2311;
- [4] F. Li, J. Zhuang, G. Jiang, H. Tang, A. Xia, L. Jaing, Y. Song, Y. Li and D. Zhu, *Chem Mater.*, 2008, **20**, 1194-1194;
- [5] V. Balzani, A. Credi, M. Venturi, *Chem. Soc. Rev.*, 2009, **38**, 1542, 1550;
- [6] H. Hamish, J. Wilkinson, *Microfluid Nanofluid* 2008, **4**, 53-79
- [7] E. A. J. Marcatili and R. A. Schmeltzer, *Bell Syst. Tech. J.* 1964, **43**, 1783 – 1809;
- [8] C. Monat, P. Domachuk and B. J. Eggleton, *Nat. Photonics*, 2007, **1**, 106 –114;
- [9] P. Anzenbacher and M. A. Palacios, *Nat. Chem. Biol.*, 2009, **5**, 80– 86;
- [10] L. Rindorf, J. B. Jensen, M. Dufva, L. H. Pedersen, P. E. Høiby and O. Bang, *Opt. Express*, 2006, **14**, 8224 –8231;
- [11] V. Horowitz, D. Awschalom and S. Pennathur, *Lab Chip*, 2008, **8**, 1856–1863;
- [12] P. Measor, B. S. Phillips, A. Chen, A. R. Hawkins and H. Schmidt, *Lab Chip*, 2011, **11**, 899–904;
- [13] P. S. J. Russell, *Journal of Lightwave Technology*, 2006, **24** 4729-4746;
- [14] C. M. Cordeiro, M. A. Franco, C. J. Matos, F. Sircilli, V. A. Serrão and C. H. Cruz, *Opt. Lett.* 2007, **32**, 3324 –3326;
- [15] Y. L. Hoo, W. Jin, H. L. Ho, D. N. Wang and R. S. Windeler, *Opt. Eng.* 2002, **41**, 8–9;
- [16] C. M. B. Cordeiro, M. A. R. Franco, G. Chesini, E. C. S. Barretto, R. Lwin, C. H. B. Cruz and M. C. J. Large, *Opt. Express*, 2006, **14**, 13056 –13066;
- [17] T. G. Euser, J. S. Y. Chen, M. Scharrer, P. S. J. Russell, N. J. Farrer, P. J. Sadler and P. St. J. Russell, *J. Appl. Phys.* 2008, **103**, 103108;
- [18] L. W. Kornaszewski, N. Gayraud, J. M. Stone, W. N. MacPherson, A. K. George, J. C. Knight, D. P. H and D. T. Reid, *Opt. Express*, 2007, **15**, 11219 – 11224;

- [19] T. Ritari, J. Tuominen, H. Ludvigsen, J. C. Petersen, T. Sørensen, T. P. Hansen and H. R. Simonsen, *Opt. Express*, 2004, **12**, 4080–4087;
- [20] J.S.Y. Chen T. G. Euser, N. J. Farrer, P. J. Sadler and P. St.J. Russell, *Chem. Eur. J.* 2010, **16**, 5607 – 5612;
- [21] A. Khetani, M. Laferrière, H. Anis and J.C. Scaiano, *J. Mater. Chem.*, 2008, **18**, 4769-4774;
- [22] K.M. Tait, J. A. Parkinson, S. P. Bates, W. J. Ebenezer and A. C. Jones., *J. Photochem. Photobiol. A: Chemistry*, 2003, **154**, 179–188;
- [23] S. R. Hairi, G. A. Taylor, and L. W. Schultz, *J. Chem. Educ.*, 1990, **67** (8), 709-712;
- [24] S. Kobayashi, H. Yokohama and H. Kamei, *Chem Phys. Lett*, 1987, **138**, 333;
- [25] M. Poprawa-Smoluch, J. Baggernam, HG. Zhang, H. P. A. Maas, L. De Cola and A. M. Brouwer, *J. Phys. Chem. A* 2006, **110**, 11926-11937;
- [26] N. A. Wazzan, P. R. Richardson and A. C. Jones, *Photochem. Photobiol. Sci.*, 2010, **9**, 968-974;
- [27] K. Gille, H. Knoll and K. Quitzsch *Int. J. Chem. Kinet.* 1999, **31**, 337–350;
- [28] H. M. D. Bandara and S. C. Burdette, *Chem Soc Rev*, 2012 DOI: 10.1039/c1cs15179g;
- [29] G. Gabor and E. Fisher, *J. Phys. Chem.*, 1971, **75**, 581–583
- [30] M. W. Mosher and J. M. Ansell, *J. Chem. Educ.*, 1975, **52**, 195-196;
- [31] K.G. Yager and C.J. Barrett, *J. Photochem. Photobiol. A: Chemistry* 2006, **182**, 250-261;
- [32] M. Irie, *Chem. Rev.* 2000, **100**, 1683-1684;
- [33] M. B. Sponsler, *Optical Sensors and Switches*, (Eds: V. Ramamurthy, K. S. Schanze), Marcel Dekker, New York and Basel, 2001, Chapter 8;
- [34] R.H. El Halabieh, O.Mermut and C.J. Barrett, *Pure Appl. Chem.* 2004, **76**, 1445-1465;
- [35] V. Balzani, A. Credi, M. Venturi, , *Pure Appl. Chem.* 2003, **75**, 541-547;
- [36] Andrew A. Beharry and G. Andrew Woolley, *Chem. Soc. Rev.*, 2011, **40**, 4422–4437;

- [37] J. Shan, S. Xu, W. Shi, L. Liu and L. Xu, "Control of Photoisomerization Quantum Efficiency by Metallic Nanostructures," in *Laser Science*, OSA Technical Digest (CD) (Optical Society of America, 2010), paper LTuA6
- [38] P. D. Wildes, J. G. Pacifici, Irick, Jr. and D. G. Whitten, *J. Am. Chem. Soc.*, 1971, **93**, 2004-2008;
- [39] T. Asano and T. Okada, *J. Org. Chem.* 1984,**49**, 4387-4391;
- [40] J. Dokic, M. Gothe, J. Wirth, M. V. Peters, J. Schwarz, S. Hecht and P. Saalfrank, *J. Phys. Chem. A* 2009, **113**, 6763–6773.